


Universality of the local persistence exponent for models in the directed Ising class in one dimensionNitesh D. Shambharkar¹ and Prashant M. Gade^{2,*}¹*Vidya Vikas Arts, Commerce and Science College, Samudrapur 442 305, India*²*Department of Physics, Rashtrasant Tukadoji Maharaj Nagpur University, Nagpur 440 033, India* (Received 21 December 2018; revised manuscript received 17 July 2019; published 12 September 2019)

We investigate local persistence in five different models and their variants in the directed Ising (DI) universality class in one dimension. These models have right-left symmetry. We study Grassberger's models A and B. We also study branching and annihilating random walks with two offspring: the nonequilibrium kinetic Ising model and the interacting monomer-dimer model. Grassberger's models are updated in parallel. This is not the case in other models. We find that the local persistence exponent in all these models is unity or very close to it. A change in the mode of the update does not change the exponent unless the universality class changes. In general, persistence exponents are not universal. Thus it is of interest that the persistence exponent in a range of models in the DI class is the same. Excellent scaling behavior of finite-size scaling is obtained using exponents in the DI class in all models. We also study off-critical scaling in some models and DI exponents yield excellent scaling behavior. We further study graded persistence, which shows similar behavior. However, for a logistic map with delay, which also has the transition in the DI class, there is no transition from nonzero to zero persistence at the critical point. Thus the accompanying transition in persistence and universality of the persistence exponent hold when the underlying model has right-left symmetry.

DOI: [10.1103/PhysRevE.100.032119](https://doi.org/10.1103/PhysRevE.100.032119)**I. INTRODUCTION**

Understanding the critical phenomena in equilibrium systems is an important triumph of theoretical physics in the past century. There have been attempts to extend a similar theory to nonequilibrium systems. We can observe a variety of phases and phase transitions in nonequilibrium systems. They range from synchronization of birds and the transition between different patterns in chemical reactions to the transition to turbulence in fluids. It is fair to say that studies in this fascinating range of phase transitions have only started. The most investigated phase transition in this respect has been the transition to an absorbing state in the various systems. Nonequilibrium systems need not obey detailed balance and it is possible for the system to be trapped in an absorbing state. Jensen and Grassberger conjectured that when there is a unique absorbing state and certain conditions are satisfied, the continuous transition is in the directed percolation (DP) universality class. The conditions are that it should have no quenched disorder and no additional symmetries, but it should have short-range interactions and a positive one-component order parameter which distinguishes between fluctuating and unique absorbing states.

Directed percolation is the most-studied universality class in nonequilibrium systems. However, there are few other reported universality classes for the transition to the absorbing state and related transitions. The parity-conserving universality class [1–3], the voter universality class [4,5], dynamical percolation [6–8], compact directed percolation [9,10], and the Manna universality class [11] have been reported [12].

In the parity-conserving universality class, the local dynamics has a certain parity and the number of particles or kinks is conserved modulo 2. At least in one dimension, it clearly shows exponents different from DP and the upper critical dimension is estimated to be $\frac{4}{3}$ [2]. This is also known as a branching and annihilating random walk (BARW) or directed Ising (DI) universality class [13]. In the voter model, each site is assigned one of, say, two opinions initially. The update consists of randomly choosing a site and assigning it the opinion of one of its randomly chosen neighbors [4,5]. In dynamic percolation, we study the generalization of directed percolation including the effect of immunization. The same universality class is obtained in models with partial immunization where the immune site can be reinfected with a lower probability than the susceptible site [14–16]. In compact directed percolation, if all neighbors of a certain site are infected, the site is infected with probability one [9,10]. This model has two absorbing states, one in which all sites are infected and the other in which there are no infected sites. In the Manna model, a given site can have an unlimited number of particles. All sites occupied by at least two particles are considered active and all particles from active sites are redistributed randomly and independently to neighboring sites. This is a locally particle-conserving model. The active particle density reaches a certain value after a transient. The active particle density is an order parameter and the particle density is a control parameter. Below the critical density, the order parameter vanishes in the steady state [11,17].

Other classes include pair contact process introduced by Jensen [18]. This is a model which has infinitely many absorbing states. A pair of sites on a d -dimensional lattice is randomly selected. If they are occupied, branching or annihilation occurs with a certain probability. Either both particles

*prashant.m.gade@gmail.com

are annihilated with probability p or a site neighboring the selected pair is chosen and a particle is created if the site is empty with probability $1 - p$. It is clear that all configurations which do not have a pair of particles are frozen states where no further evolution can occur. Now it is fairly established that even though the Janssen-Grassberger conjecture does not apply here, this process is in the DP universality class. Another version of the above process is known as the pair contact process with diffusion. It has been subjected to several investigations [19–22]. In this process, particles are allowed to diffuse and two possible absorbing states, namely, an empty lattice and a solitary diffusing particle, exist in this model. There is a special case known as tricritical directed percolation [23,24], in which there are points where the first-order and second-order transitions meet. The transitions show a different critical behavior, which is reported in dimension $d > 1$. [In a one-dimensional (1D) system, the surface tension does not depend on the domain size and first-order transitions to a fluctuating state do not occur.]

The universality classes are identified by critical exponents which are characteristic of a given class of phase transitions. They depend only on dimensionality and symmetries, and the same exponents have been found in seemingly disparate systems. Absorbing phase transitions are characterized by four (or three in the presence of certain symmetry) critical exponents.

Recently, another exponent, known as the persistence exponent, related to the first-passage time has been reported. This a non-Markovian quantity and the local persistence exponent θ_l (denoted by θ in this work) is obtained by finding the number of sites which have not deviated from the initial state even once until a certain time. Another quantity, the global persistence exponent θ_g , is also defined and it is obtained by measuring configurations in which the order parameter has not crossed its average value until a certain time [25]. This exponent is found to satisfy the relationship $\theta_{gz} = \lambda - d + 1 - \eta/2$, where η is the static and λ the autocorrelation exponent. This relationship can be derived under the assumption that the dynamics of the global order parameter is Markovian [26]. Thus θ_g can be expressed in terms of other exponents, while no such relationship has been found for θ_l . There are numerous counterexamples to show that θ_l is not universal (see [19]). These examples will be discussed in the next section. We study the parity-conserving universality class in one dimension, which has more than one absorbing state linked by symmetry. This is known as the directed Ising class [13]. Apart from completing the study of the local persistence exponent in the directed Ising class, our work shows reasonable evidence that the persistence exponent is universal and has value unity or very close to it in a range of models.

The models in the DI universality class can be broadly classified according to the mode of the update. The update rule is a parallel update for Grassberger’s models A and B, while it is a random sequential update for branching and annihilating random walks and interacting monomer-dimer models. For the nonequilibrium kinetic Ising model, sites from the even sublattice are chosen randomly and updated followed by a random sequential update of sites from the odd sublattice. We also consider a variant in which all sites of the even

lattice are updated followed by the entire odd sublattice. These models will be defined in detail in the next section. Finally, we consider a logistic map with a delay which is found to have the transition in the DI universality class. In this case, the update is carried out in a deterministic sequential manner from left to right in typewriter mode [27]. In this case, there is no transition in persistence from a nonzero to a zero value at the critical point. Thus there is no well-defined persistence exponent in this case.

II. MODELS

A. Probabilistic cellular automata models A and B

Grassberger *et al.* [28,29] studied two 1D models of cellular automata in which the number of kinks between ordered states is conserved modulo 2. Each site is in a state 0 or 1. The value of the central site evolves according to its value as well as that of its nearest neighbors. Model A evolves with rule number 94 in the notation of Wolfram [30], except for the 110 and 011 configurations, where the central spin 1 flips to 0 with probability p and remains unchanged otherwise. Model B evolves with Wolfram’s rule number 50, except for the 110 and 011 configurations, where the central spin 1 does not change value with probability p and flips otherwise. Historically, these are first instances of models which are clearly not in the DP universality class. There are two equivalent absorbing states in both models. The states (1010...) and (0101...) are absorbing states in both models. In model A they are frozen absorbing states while in model B the asymptotic state is periodic with period 2 and we observe oscillations between the (1010...) and (0101...) states asymptotically. For clarity, we have tabulated the governing rules for models A and B in Table I. This absorbing phase transition is unambiguously in a different universality class than DP and this universality class is known as the DI universality class.

B. Branching annihilating random walk with two offsprings

The branching annihilating random walk was introduced by Bramson and Gray [31]. We will be studying the two-offspring BARW (BARW2). (The universality class depends on the number of offsprings.) In this model, a site is picked at random. If the site is occupied, it undergoes nearest-neighbor diffusion with probability p and it may branch with the rate $1 - p$. Nearest-neighbor diffusion occurs in a random direction. If the target site is occupied, both particles are annihilated. Similarly, if a branching attempt is selected, the unoccupied nearest neighbors are occupied. If a newly created particle is placed on a previously occupied site, both particles are removed.

C. Interacting monomer-dimer model

The interacting monomer-dimer (IMD) model is a generalization of the simple monomer-dimer model [32–34]. A monomer A is deposited on a random site i of the lattice provided its nearest neighbors $i + 1$ or $i - 1$ do not contain A . Similarly, a dimer B_2 is deposited on a pair of vacant sites i and $i + 1$ provided its nearest neighbors $i + 2$ or $i - 1$ do not contain B . The simulation proceeds as follows. A monomer A

TABLE I. Grassberger's models A and B. Here prob. denotes probability.

Model A		Model B	
t	$t + 1$	t	$t + 1$
111	0	111	0
101	0	101	1
010	1	010	0
100	1	100	1
001	1	001	1
011	0 with prob. p , 1 with prob. $1 - p$	011	1 with prob. p , 0 with prob. $1 - p$
110	0 with prob. p , 1 with prob. $1 - p$	110	1 with prob. p , 0 with prob. $1 - p$
000	0	000	0

is adsorbed at a random site on the 1D lattice with probability $(1 - s)p$ and a dimer B_2 with probability $(1 - s)(1 - p)$. With probability s , a single B located at that site from the lattice is removed. (If there is another B on the nearest site, we remove it as well. Allowing removal of a single B is essential so that the absorbing state does not change.) We choose $s = 0.5$. Note that the rules allow for A to be deposited near B and vice versa. There are no nearest-neighbor restrictions here. However, whenever A is deposited near B or one B of the dimer B_2 is deposited near A , the dimer B_2 dissociates and the AB product immediately leaves the lattice. It is clear that $(A0A0\dots)$ or $(0A0A\dots)$ are absorbing states of this system. These states have the only monomer at the odd- or even-numbered lattice sites and vacancy otherwise. No pair of adjacent vacant sites exists in this state, so a dimer cannot be adsorbed. Furthermore, all vacant sites have A as a neighbor, so a monomer cannot be adsorbed either. These are absorbing states where no further deposition is possible.

D. Nonequilibrium kinetic Ising model

The nonequilibrium kinetic Ising model (NEKIM) was proposed by Menyhárd [35]. It combines spin-flip dynamics at $T = 0$ and spin-exchange dynamics at $T = \infty$. The spin-flip part is applied using two sublattices updating and is followed by an exchange of neighboring spins with probability p_{ex} which is fixed at 0.3. A spin flip is carried out alternately at even and odd sublattices with certain probability. This probability depends on the spin values at a given site and its nearest neighbors. When a central spin has the same value as neighboring spins the probability of the spin flip is given by p_{same} . When both neighbors have opposite spin, it is given by p_{opposite} . When neighbors have opposite signs, it is given by $p_{\text{indifferent}}$. We choose their values to be $p_{\text{same}} = \Gamma(1 + \delta)(1 - \gamma)/2$, $p_{\text{opposite}} = \Gamma(1 + \delta)(1 + \gamma)$, and $p_{\text{indifferent}} = \Gamma(1 - \delta)/2$, where $\Gamma = 0.35$, $\delta = -0.395$, and $\gamma = 1$, as in the original formulation. Note that $p_{\text{same}} = 0$. Thus the state with all up spins or the state with all down spins is an absorbing state. (The probability p_{same} is the probability of the creation of kink pairs inside the ordered domains at $T \neq 0$.) From the above description, it is clear that a kink separating two domains can carry out random walks with probability $2p_{\text{indifferent}}$ and two kinks getting into neighboring positions will annihilate with probability $2p_{\text{opposite}}$.

We note that the behavior of global persistence has been studied in this model. The exponent for global persistence

is found to be 0.67. Menyhárd and Odor have shown that finite-size scaling at the critical point for the NEKIM has the same exponent 1.75 as the one for the order parameter [25].

E. Nonequilibrium kinetic Ising model with parallel update

In the above model, first, $N/2$ sites on the even sublattice are randomly chosen and updated, which is followed by an update of $N/2$ randomly chosen sites on the odd sublattice. Thus certain lattice sites may not be updated at all. Now we consider a variant in which all sites on the even sublattice are updated followed by an update of all sites on the odd sublattice. The critical value of δ is now given by $\delta = -0.249$. We have kept other values fixed. At the critical value, the order parameter decays with exponent $\delta = 0.28(3)$. Thus the transition is still in the DI universality class. We will discuss the persistence exponent of all the above models in the next section.

We may consider a variant in which all sites are updated synchronously. This model belongs to a different universality class. The order parameter decays with the exponent 0.5 and the persistence decays with the exponent 0.38, which is very close to $\frac{3}{8}$. This is a Glauber-Ising universality class [36–38]. We have found that changing the mode of the update may result in a change of the universality class to the Glauber-Ising class in models other than the NEKIM such as coupled maps and Grassberger's models. Obviously, this results in a change of exponents. Though a change in universality class due to a change in the mode of update is an interesting topic in itself, in this work we focus and present results only on systems which show a transition in the DI class (see also [39]).

III. PERSISTENCE IN DIRECTED ISING MODELS

The persistence problem is an analog of first-passage problems in the stochastic system and the exponent thus obtained is a critical exponent unrelated to previous critical exponents. It is rather difficult to compute analytically even in the simplest cases such as the diffusion equation. The reason is that it depends on the entire history and is a non-Markovian quantity. Various definitions of persistence such as local persistence, global persistence, and block persistence have been proposed. Though initial studies have been in discrete systems such as spin systems, suitably modified generalizations have been proposed in systems with a continuous-variable value such as coupled maps. The most widely studied quantity is the local persistence probability $P(t)$ [also denoted by $P_l(t)$ in the

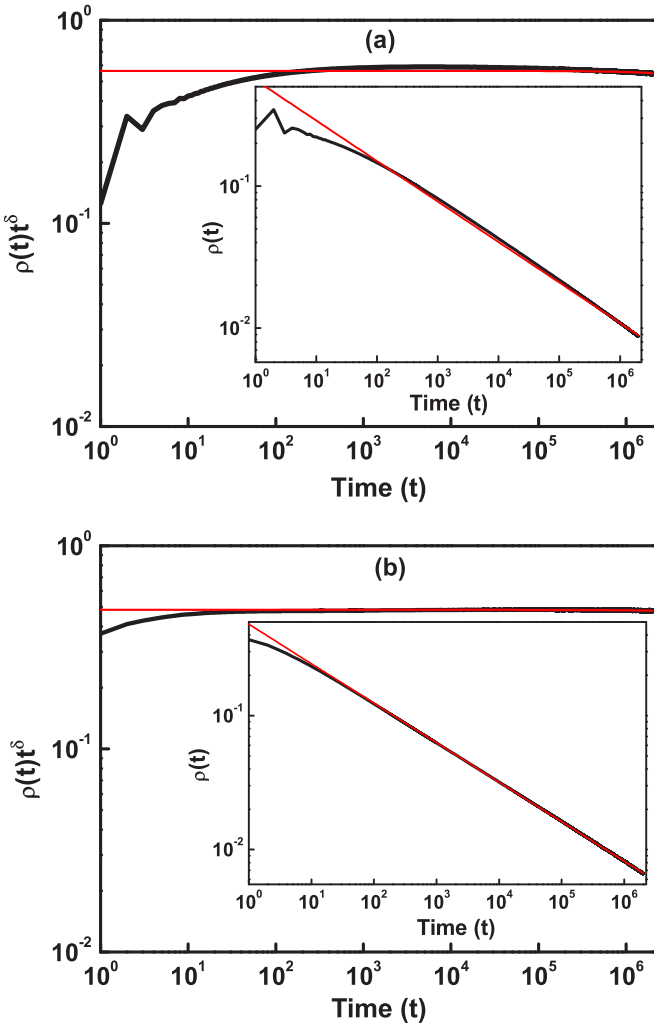


FIG. 1. (a) Plot of $\rho(t)t^\delta$ as a function of time t with $\delta = 0.285$ at the critical point $p_c = 0.1237$ for Grassberger's model A. The inset shows the order parameter $\rho(t)$ as a function of time t at the critical point. (b) Order parameter $\rho(t)t^\delta$ with $\delta = 0.295$ plotted as a function of time t at the critical point $p_c = 0.5425$ for Grassberger's model B. The inset shows the order parameter $\rho(t)$ as a function of time t at the critical point. We carry out simulations for $N = 1 \times 10^6$ sites and average over 1×10^3 configurations.

literature]. It is defined as the probability that a local variable at a given point in space has not changed its state until time t during stochastic evolution. It is observed that, in several systems, at the critical point, the local persistence probability decays algebraically as

$$P(t) \sim t^{-\theta_l}. \tag{1}$$

The exponent θ_l is known as a local persistence exponent. (We will refer to it as the persistence exponent θ in this work). In spin systems, the local persistence at time t , $P(t)$, is the fraction of sites which did not change their initial spin state at all times $t \leq T$. It may show a power-law decay at zero temperature for Ising- or Potts-type systems. A similar exponent is defined for nonequilibrium models such as directed percolation. The persistence exponents themselves are not universal and depend on the delicate details of evolution.

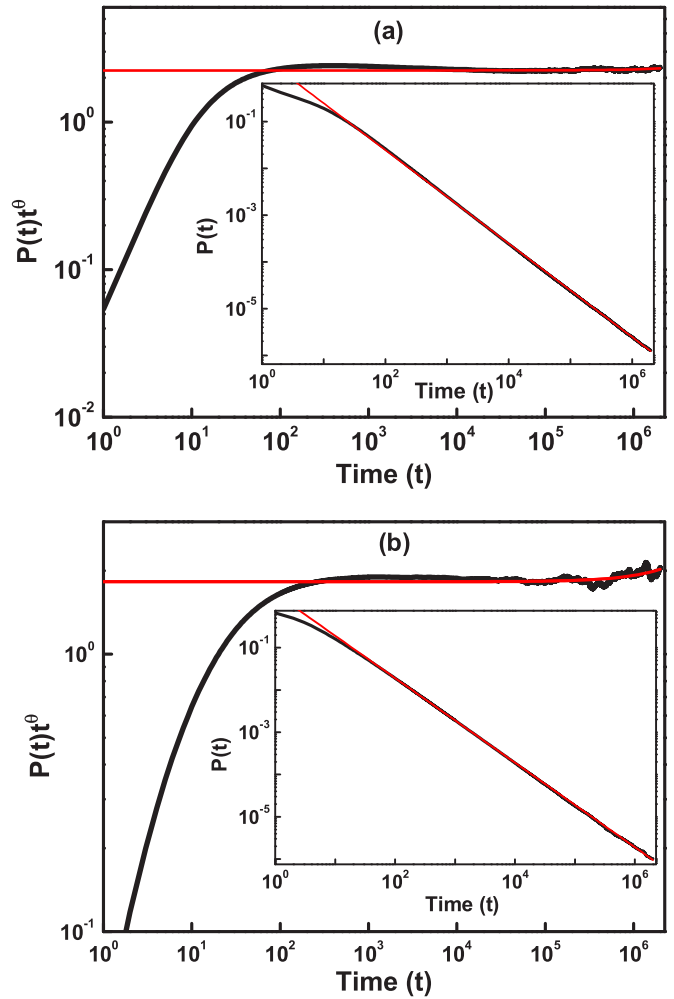


FIG. 2. (a) Plot of $P(t)t^\theta$ as a function of time t with $\theta = 0.99(4)$ at the critical point $p_c = 0.1237$ for Grassberger's model A. The inset shows $P(t)$ as a function of time t at the critical point. (b) Plot of $P(t)t^\theta$ as a function of time t using $\theta = 1.00(0)$ at the critical point $p_c = 0.5425$ for Grassberger's model B. The inset shows $P(t)$ as a function of time t at the critical point. We carry out simulations for $N = 1 \times 10^6$ sites and average over 1×10^3 configurations.

Models in the same universality class have the same persistence exponent in some cases, but not necessarily so. The persistence exponent of widely different models such as the 1D Ising model, coupled logistic maps, and the Sz-najd model is $\frac{3}{8}$ [38,40,41]. Similarly, it has been observed that the persistence exponent in 1D DP models such as the Domany-Kinzel model [42], Ziff-Gulari-Barshad model [43], site percolation [44], and 1D coupled circle maps is the same, i.e., $\frac{3}{2}$ or very close to it [45]; however, later studies established that the persistence exponents can widely differ for models in the same universality class. The exponent is not universal. (The value of exponents ranges from 1.5 to 2.24 for models in the 2D DP universality class.) Despite its nonuniversality, the precise value may be of interest from the viewpoint of detailed dynamics. We argue that even if the persistence exponent is not universal, it can help in finding other universal exponents. Again, if a large fraction of models in a given universality class has the same persistence

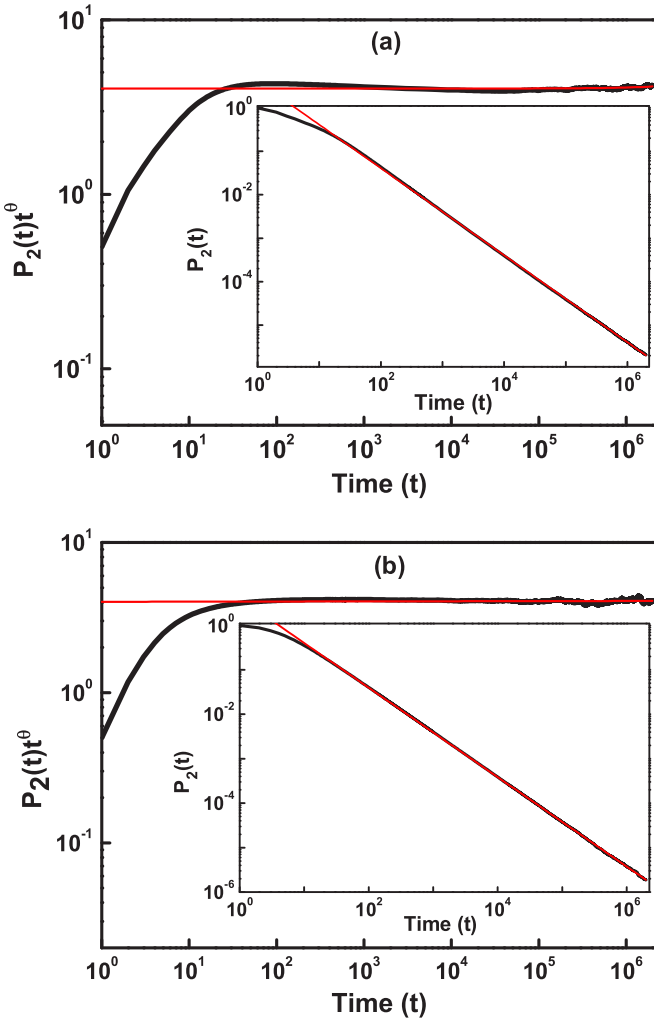


FIG. 3. (a) Plot of $P_2(t)t^\theta$ as a function of time t with $\theta = 1.00(0)$ at the critical point $p_c = 0.1237$ for Grassberger's model A. The inset shows $P_2(t)$ as a function of time t at the critical point. (b) Plot of $P_2(t)t^\theta$ as a function of time t with $\theta = 1.00(5)$ at the critical point $p_c = 0.5425$ for Grassberger's model B. The inset shows $P_2(t)$ as a function of time t at the critical point. We carry out simulations for $N = 1 \times 10^6$ sites and average over 1×10^3 configurations.

exponent, it is an interesting subclass. In this work, persistence in 1D DI models is studied and the persistence exponent is close to unity in all cases. We believe that this nontrivial exponent sheds further light on the detailed dynamical nature of phase transitions. There can be cases when the order parameter is not easily identified. The scaling behavior of persistence can shed light on other exponents in the system. We give examples and make a detailed argument in the next section.

Fuchs *et al.* defined a quantity graded persistence $P_k(t)$ which is a fraction of sites activated less than k times until time t . We compute this quantity in a few models. The exponent obtained in this case is almost the same as the persistence exponent and has similar scaling properties [44]. If the exponent is the same, ratios $P_k(t)/P(t)$ can help us to find the error in the persistence exponent.

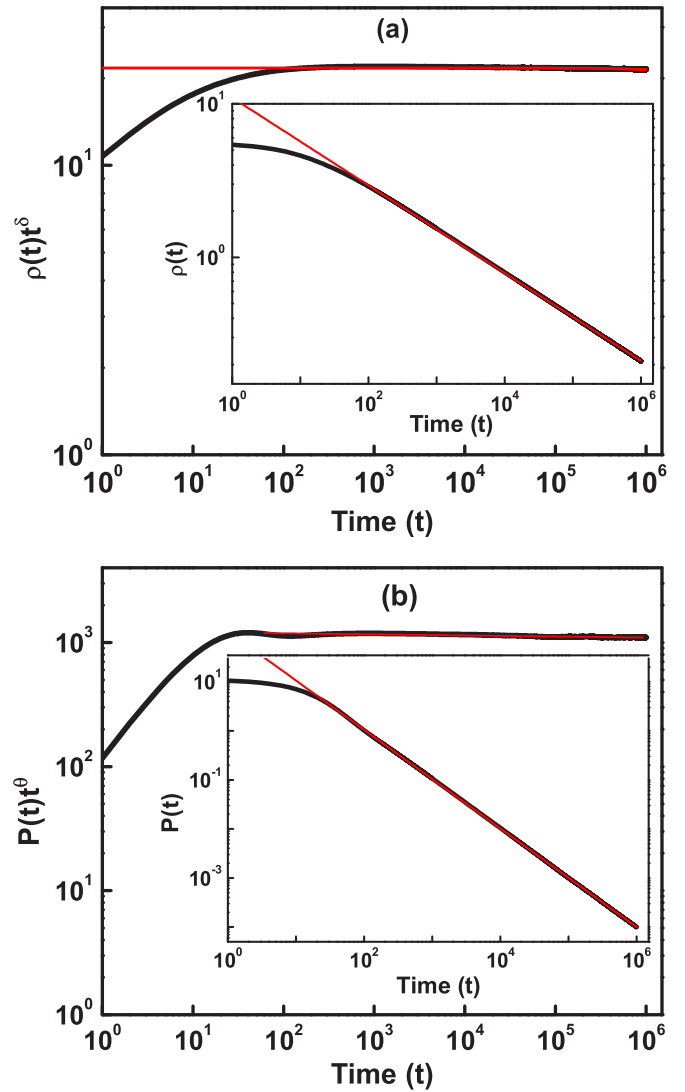


FIG. 4. (a) Plot of $\rho(t)t^\delta$ as a function of time t using $\delta = 0.28(5)$ at the critical point $p_c = 0.5108$ for the BARW2 model. The inset shows the order parameter $\rho(t)$ as a function of time t at the critical point. (b) Plot of $P(t)t^\theta$ as a function of time t using $\theta = 1.00(5)$ at the critical point $p_c = 0.5108$ for the BARW2 model. The inset shows $P(t)$ as a function of time t at the critical point. We carry out simulations for $N = 2 \times 10^4$ sites and average over 8×10^3 configurations.

IV. SIMULATION AND RESULTS

In Grassberger's models, the initial state is chosen to be 0 or 1 with equal probability. In the NEKIM, it is chosen to be spin up or down with equal probability. In the IMD model, we start with a flat surface, while in the BARW2 model, sites are empty or occupied with equal probability in the beginning. For Grassberger's models A and B, Grassberger has estimated critical points as $p_c = 0.13 \pm 0.02$ and 0.5403 ± 0.0013 , respectively. We estimate p_c as 0.1237 and 0.5425 for models A and B, respectively. For these values, the order parameter decays as $t^{-\delta}$, with $\delta = 0.285$ and 0.295 for models A and B, respectively. The behavior of the order parameter $\rho(t)$ as well $\rho(t)t^\delta$ is shown in Figs. 1(a) and 1(b) at the critical

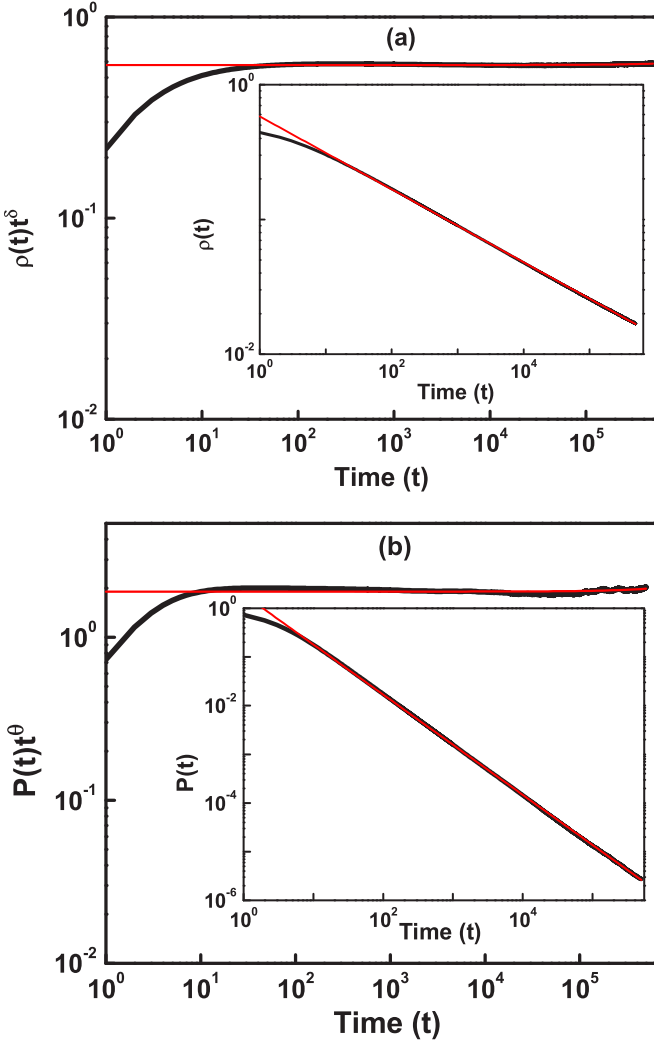


FIG. 5. (a) Plot of $\rho(t)t^\delta$ as a function of time t using $\delta = 0.27(0)$ at the critical point $\delta_c = 0.395$ for the NEKIM. The inset shows the order parameter $\rho(t)$ as a function of time t at the critical point. (b) Plot of $P(t)t^\theta$ as a function of time t using $\theta = 1.02(9)$ at the critical point $\delta_c = 0.395$ for the NEKIM. The inset shows $P(t)$ plotted as a function of time t at the critical point. We carry out simulations for $N = 2 \times 10^6$ sites and average over 2×10^2 configurations.

point and an excellent power law is obtained over six decades. This value of δ is in close agreement with values for the DI class, where it is estimated to be 0.27–0.29. The simulations are carried out for system size $N = 10^6$ and are averaged over 10^3 configurations. At the critical point, we compute the persistence as well as graded persistence for the above models. For model A, the persistence exponent is found to be 0.99(4) [Fig. 2(a), inset], while for model B, it is found to be 1.00(0) [Fig. 2(b), inset]. These exponents are found by fitting the power laws using standard software such as ORIGIN. They are further confirmed by plotting $P(t)t^\theta$ as a function of t . We find a clear flat line asymptotically in this graph. The behavior of persistence $P(t)$ as well as for $P(t)t^\theta$ is shown in Figs. 2(a) and 2(b) for both models A and B.

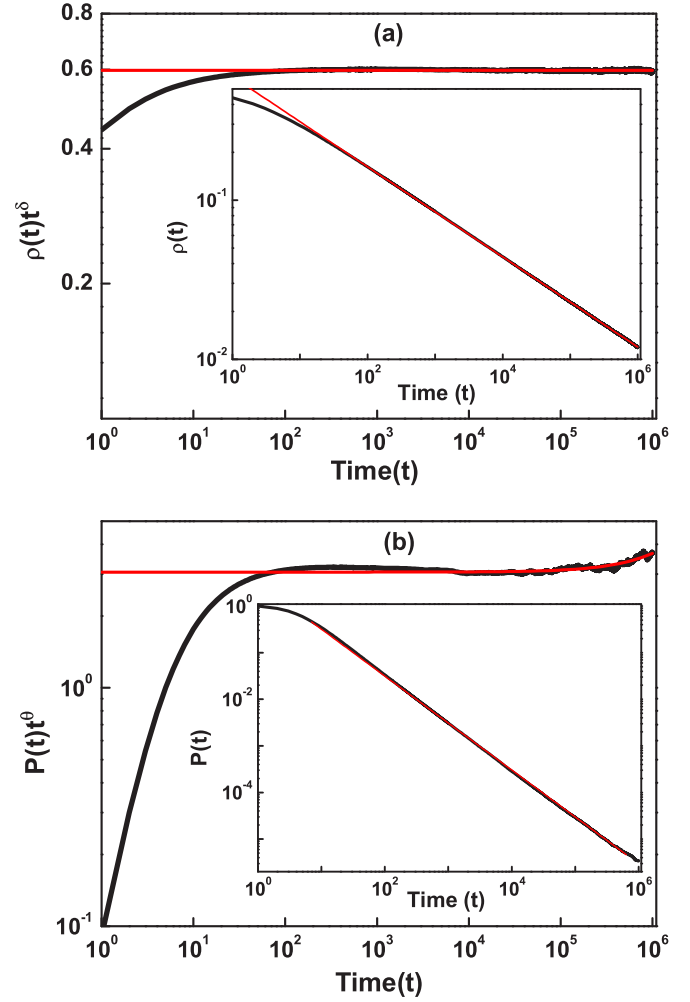


FIG. 6. (a) Plot of $\rho(t)t^\delta$ as a function of time t using $\delta = 0.28(3)$ at the critical point $p_c = 0.249$ for the parallel update NEKIM. The inset shows the order parameter $\rho(t)$ as a function of time t at the critical point. (b) Plot of $P(t)t^\theta$ as a function of time t using $\theta = 1.00(6)$ at the critical point $p_c = 0.249$ for the parallel update NEKIM. The inset shows $P(t)$ plotted as a function of time t at the critical point. We carry out simulations for $N = 1 \times 10^6$ sites and average over 1×10^3 configurations.

We also find graded persistence $P_2(t)$ for model A as well as model B. The persistence exponent for graded persistence $P_2(t)$ is found to be 1.00(0) for model A and 1.00(5) for model B. Again, they are confirmed by plotting $P_2(t)t^\theta$ as a function of t . The behavior of graded persistence at the critical point for Grassberger’s model A and B is shown in Figs. 3(a) and 3(b).

We simulate branching annihilating random walks with two offsprings. The critical point is estimated $p_c = 0.5054$ in Ref. [1]. We simulate the BARW2 model for system size 2×10^4 and average over 10^3 configurations. We estimate $p_c = 0.5108$, at which the order parameter $\rho(t)$ scales as $t^{-\delta}$ with $\delta = 0.28(5)$. The persistence exponent is obtained as 1.00(5) for this model. The behavior of the order parameter $\rho(t)$ and persistence $P(t)$ for the BARW2 model is shown in Figs. 4(a) and 4(b), respectively.

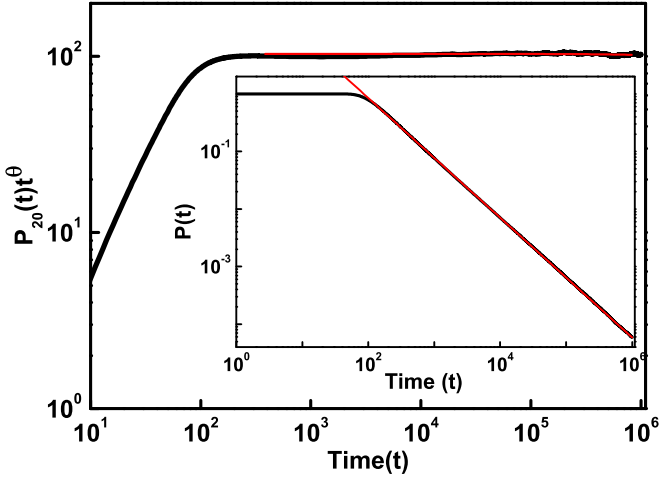


FIG. 7. Plot of $P_{20}(t)t^\theta$ as a function of time t using $\theta = 1.04$ at the critical point $p_c = 0.249$ for the 20-site parallel update NEKIM. The inset shows $P_{20}(t)$ plotted as a function of time t at the critical point. We carry out simulations for $N = 1 \times 10^6$ sites and average over 1×10^3 configurations.

The critical point of the NEKIM was estimated to be $\delta_c = 0.395$ by Menyhárd and Ódor [46]. We simulate for lattice size 2×10^6 and average over 10^2 configurations. The order parameter decays as a power law with $\delta = 0.27(0)$ for $\delta_c = 0.395$. At this value, the persistence exponent is obtained to be $1.02(9)$, which is again very close to unity. The behavior of the order parameter and persistence for the NEKIM is shown in Figs. 5(a) and 5(b), respectively.

We also study persistence in the NEKIM with a parallel update. (We study the version in which all odd sites are updated in parallel followed by all even sites.) As mentioned above, this model falls in the DI class. The exponent δ for the order parameter is $0.28(3)$, while the persistence exponent $\theta = 1.00(6)$ in this case [see Figs. 6(a) and 6(b)]. We note that with a fully synchronous update, the universality class and persistence exponent change. We also compute $P_{20}(t)$ as a function of time and it shows an exponent of 1.04 , which is very close to unity (Fig. 7).

We simulate the IMD model for 1×10^6 sites and average over 250 configurations. The critical point of the IMD was estimated to be $p_c = 0.5325$ by Park and Park [33]. We estimate $p_c = 0.5330$ at which the order parameter $\rho(t)$ decays as $t^{-\delta}$ with $\delta = 0.27(2)$. We obtain the persistence exponent to be $1.05(4)$ in this case. The behavior of the order parameter and persistence is shown in Figs. 8(a) and 8(b).

Finite-size scaling and off-critical simulations

As mentioned above, the persistence exponent can be useful in finding other exponents of the system. We have carried out finite-size scaling and off-critical simulations in a few cases to demonstrate the usefulness of persistence in finding other exponents. There is reasonable numerical evidence now that finite-size scaling and off-critical scaling of persistence are dictated by the same exponents as that of the order parameter.

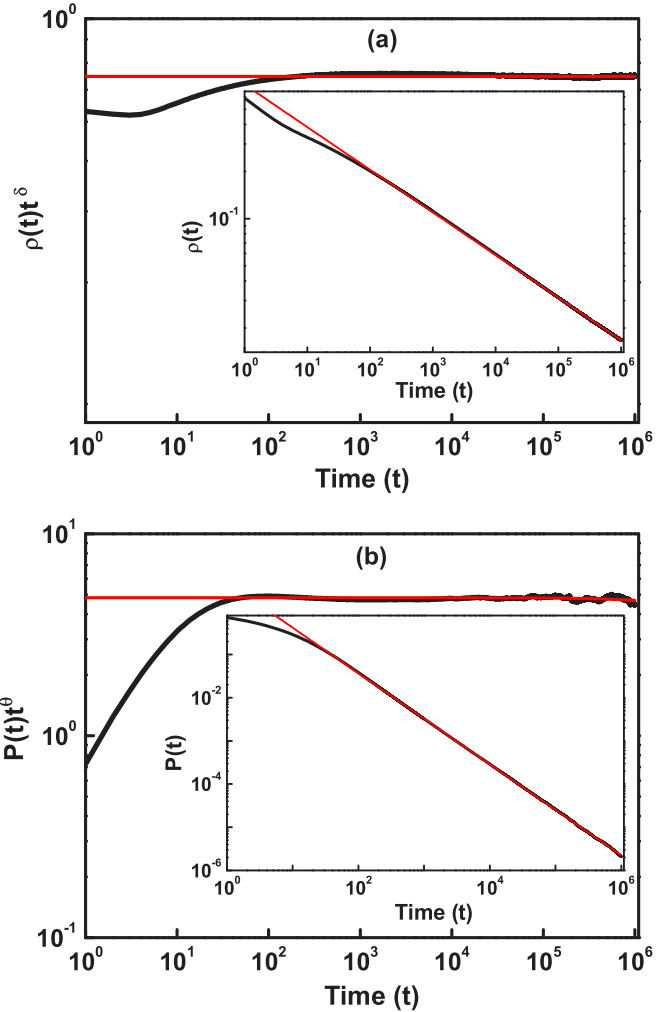


FIG. 8. (a) Plot of $\rho(t)t^\delta$ as a function of time t using $\delta = 0.27(2)$ at the critical point for the IMD model. The inset shows the order parameter $\rho(t)$ as a function of time t at the critical point. (b) Plot of $P(t)t^\theta$ as a function of time t using $\theta = 1.05(4)$ at the critical point for the IMD model. The inset shows $P(t)$ plotted as a function of time t at the critical point. We carry out simulations for $N = 1 \times 10^6$ sites and average over 250 configurations.

Some examples supporting the above conjecture are as follows. (a) Fuchs *et al.* studied the one-dimensional DP transition using the contact process as the model [44]. They obtained successful data collapse of the persistence for finite-size scaling as well as off-critical simulations using the 1D DP exponents ν_{\parallel} and z . (b) It is known that the transition to spatiotemporal intermittency in coupled circle maps in one dimension is in the DP class. Here finite-size scaling yields an exponent which matches with standard DP values [45]. (c) Persistence in Domany-Kinzel automata was studied by Hinrichsen and Koduvely. They noted that the persistence obeys finite-size scaling with the same exponents as in DP [42]. (d) Directed percolation in two dimensions has been studied. An evolutionary model of the prisoners dilemma on the 2D lattice has been investigated [47]. In a few variants of this model, successful scaling collapse for off-critical simulations has been obtained, giving the value of ν_{\parallel} which

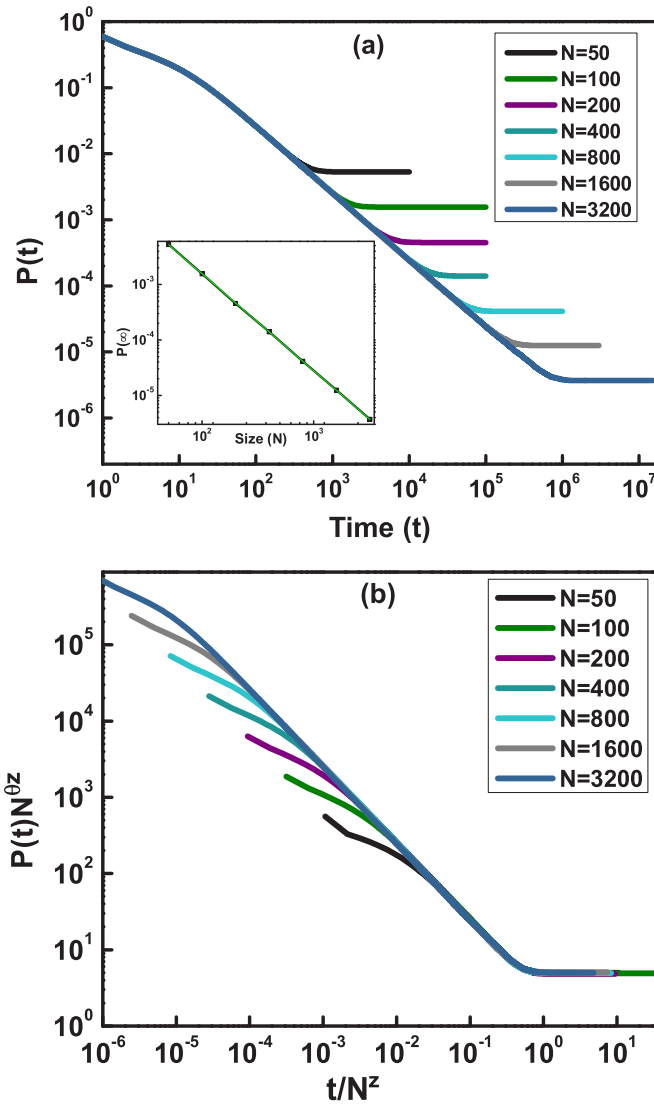


FIG. 9. (a) Plot of $P(t)$ as a function of time t at the critical point $p_c = 0.1237$ for different sizes of Grassberger's model A. The inset shows the saturation value of $P(t)$ for different sizes vs size N . (b) Plot of $P(t)N^{\theta_z}$ as a function of t/N^z with $z = 1.74(5)$ at the critical point $p_c = 0.1237$ for Grassberger's model A.

matches with the 2D DP value. (e) The Glauber-Ising model in one to four dimensions has been studied by Manoj and Ray. They observed excellent finite-size scaling collapse and the exponent matches with standard values [48]. (f) In studies on persistence in the pair contact process with diffusion, a limiting case of the pair contact process is known to be in the directed percolation universality class. Matte and Gade have carried out finite-size scaling as well as off-critical simulations in this case. The exponents $\nu_{||}$ and z match with standard DP values in this case [19].

Apart from this empirical evidence, we present a simple argument on why we expect finite-size scaling and off-critical exponents for the order parameter and persistence to be the same. Persistence saturates when the frozen state is reached and there is no further activity. The time required to reach a frozen state and for saturation of persistence should scale in

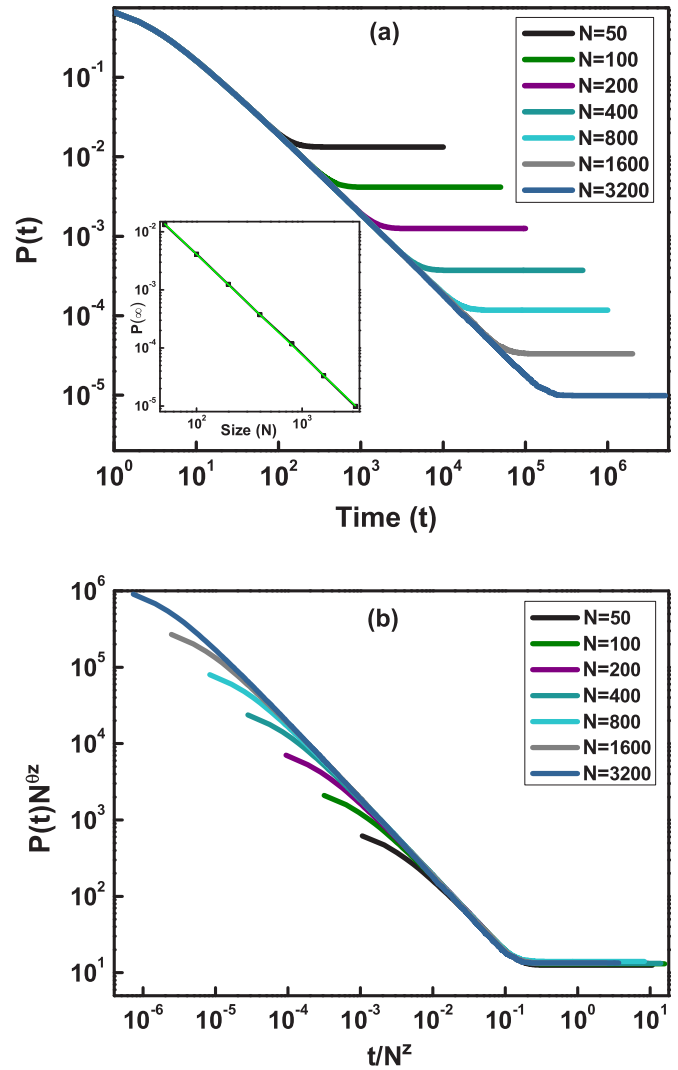


FIG. 10. (a) Plot of $P(t)$ as a function of time t at the critical point $p_c = 0.5425$ for different sizes of Grassberger's model B. The inset shows the saturation value of $P(t)$ for different sizes vs size N . (b) Plot of $P(t)N^{\theta_z}$ as a function of time t/N^z using $z = 1.75$ at the critical point $p_c = 0.5425$ for Grassberger's model B.

the same manner. If the time taken to reach a frozen state for size N scales as N^z , we expect the same time for scaling for persistence. Similarly, if on one side of the critical point the time required to reach the frozen state scales as $|p - p_c|^{-\nu_{||}}$, the time required for saturation of persistence will scale in the same manner. The asymptotic value of persistence should be $N^{-z\theta}$ or $|p - p_c|^{\nu_{||}\theta}$. The argument does not extend to the case when an active state is reached asymptotically. It would be surprising if this case yields another independent exponent. In fact, we find the same exponent even in this case.

We study finite-size scaling for persistence in all the above models. We find an excellent match with the expected DI value z in the range 1.73–1.75.

We obtain finite-size scaling using persistence $P(t)$ in models A and B. We have observed that the saturation value scales as $N^{-z\theta} \sim N^{-z}$ with $z = 1.74(5)$ and $1.73(3)$ for models A and B as we go from $N = 50$ to 3200 as shown in Figs. 9 and

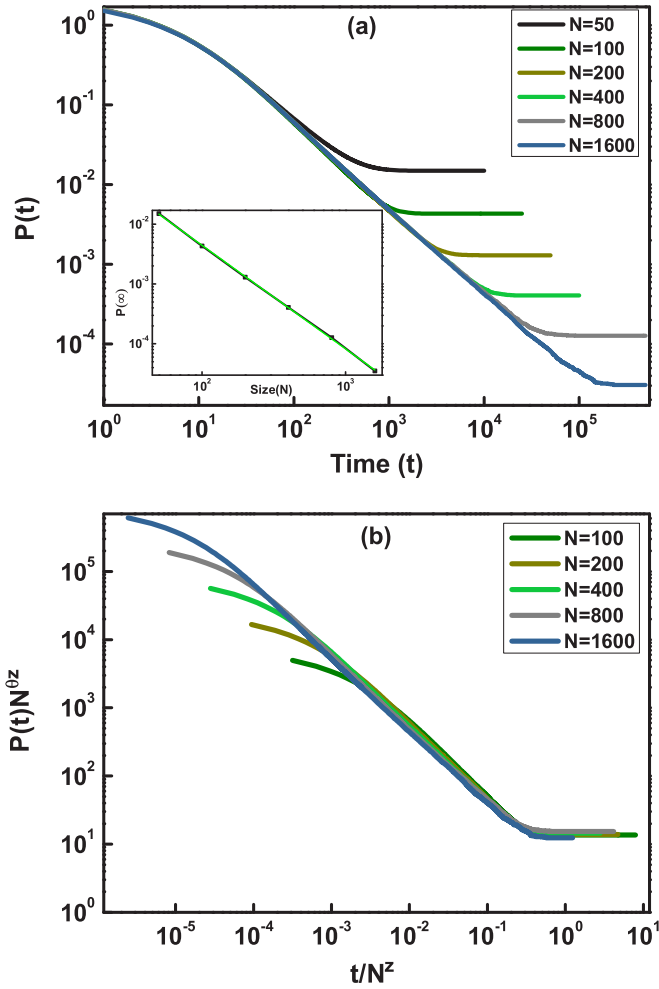


FIG. 11. (a) Plot of $P(t)$ as a function of time t at the critical point $p_c = 0.5330$ for different sizes of interacting monomer and dimer. The inset shows the saturation value of $P(t)$ for different sizes vs size N . (b) Plot of $P(t)N^{0.72}$ as a function of t/N^2 with $z = 1.72(9)$ at the critical point $p_c = 0.5330$ for the IMD model.

10. This value is in excellent agreement with the known value of z , which is 1.73–1.75 for the DI class [49–51].

We obtain finite-size scaling for persistence in the IMD model. The saturation value scales as $N^{-z\theta} \sim N^{-z}$ with $z = 1.73$ for the IMD model. The finite-size scaling for sizes ranging from $N = 50$ to 1600 is shown in Figs. 11(a) and 11(b). For the BAW2 model, we plot the saturation value of persistence from $N = 50$ to 800 and the saturation value scales as $N^{-z\theta}$ with $z = 1.72(9)$. The scaling is shown in Fig. 12 [49–51].

We also observed finite-size scaling using persistence $P(t)$ in the NEKIM. However, only surviving configurations are considered for finite-size scaling in Ref. [52]. We subtract the asymptotic value of persistence which will correspond to configurations which reach the absorbing state. An excellent scaling collapse is obtained for $z = 1.73$ (see Fig. 13).

We find persistence for values of p below and above the critical point for very large system sizes $N = 10^5$. The persistence goes to zero in the active state ($p < p_c$) and saturates to a finite value in the absorbing state ($p > p_c$). Scaling collapse

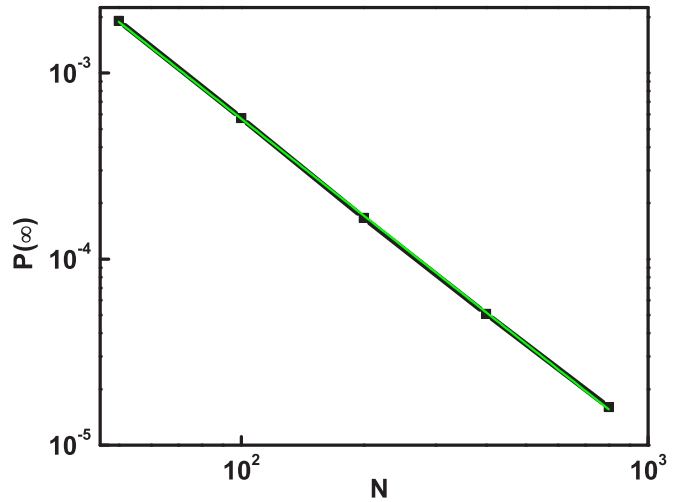


FIG. 12. Saturation value of $P(\infty)$ plotted as a function of size N at the critical point $p_c = 0.5108$ for the BAW2 model. The fitted line is proportional to N^{-z} with $z = 1.72(9)$.

of these off-critical simulations can be obtained by taking the standard value of the DI class of $\nu_{\parallel} = 3.25$. For Grassberger’s model A, we average over 10^3 initial conditions for $p < p_c$ and at least 2×10^4 initial conditions for $p > p_c$ for $N = 10^5$. For model B, we average over 10^3 initial conditions for $p < p_c$ and at least 2×10^4 initial conditions for $p > p_c$ for $N = 10^6$. We plot $P(t)\Delta^{-\theta\nu_{\parallel}}$ as a function of $t\Delta^{\nu_{\parallel}}$ where $\Delta = |p - p_c|$. An excellent scaling collapse is obtained over a range of values of Δ . The scaling collapse is shown in Figs. 14(a) and 14(b). For the IMD model, we average over 10^3 initial conditions for $p > p_c$ and at least 2×10^4 initial conditions for $p < p_c$ for $N = 10^5$. We plot $P(t)\Delta^{-\theta\nu_{\parallel}}$ as a function of $t\Delta^{\nu_{\parallel}}$, where $\Delta = |p - p_c|$. Again, scaling collapse is obtained for $\nu_{\parallel} = 3.25$, which is shown in Fig. 15. In almost all plots of persistence, a clean power law is obtained and nonlinear corrections are very weak in persistence compared to the order parameter. There is reasonable evidence to indicate that the

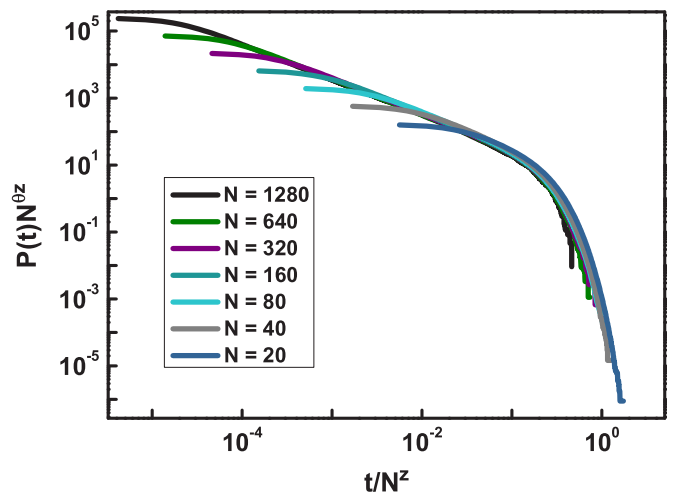


FIG. 13. Plot of $P(t)N^{0.73}$ as a function of t/N^2 with $z = 1.73$, at the critical point $\delta_c = 0.395$ for different sizes of the NEKIM. We subtract $P(\infty)$ from $P(t)$.

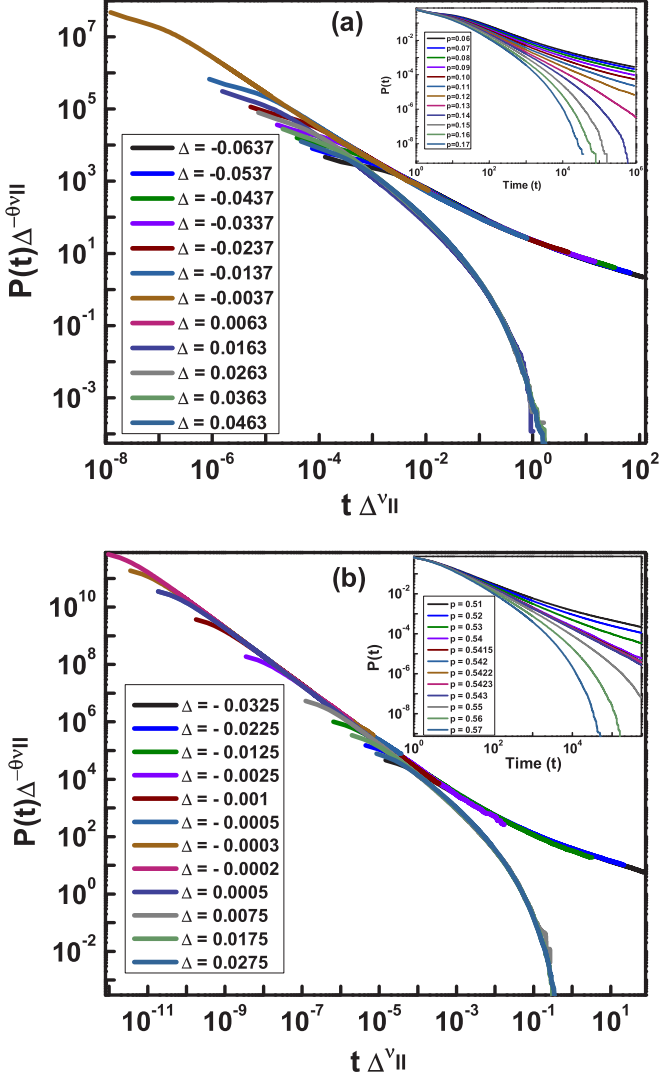


FIG. 14. (a) Plot of $P(t)\Delta^{-\theta v_{||}}$ as a function of $t\Delta\theta_{||}^v$ for Grassberger's model A at the critical point $p_c = 0.1237$ for various values of Δ . (b) Plot of $P(t)\Delta^{-\theta v_{||}}$ as a function of $t\Delta\theta_{||}^v$ for Grassberger's model B at the critical point $p_c = 0.5425$ for various values of Δ .

persistence exponent in all the above models belonging to the DI class is unity or very close to it.

We propose one more way to get an idea of the strength of nonlinear correction terms. We have found graded persistence $P_k(t)$ in some cases and it behaves in the same way as $P(t)$. Hence we propose the behavior $P(t) = ct^{-\theta}(1 + dt^{-\gamma} + \dots)$ and $P_k(t) = c_k t^{-\theta}(1 + d_k t^{-\gamma} + \dots)$. Now $P_k(t)/P(t) \sim (c_k/c)(1 + d_k t^{-\gamma})(1 + dt^{-\gamma})^{-1} \sim (c_k/c)[1 + (d_k - d)t^{-\gamma} + \dots]$. If we plot $P_k(t)/P(t)$ as a function of t , it is flat and the value of γ is almost zero. Thus the correction is not discernible. This plot is given in Fig. 16. In all cases above, we have also plotted $P(t)t^\theta$ and the graph is flat with a slope of the order of 10^{-3} with error 10^{-4} in most cases. Hence we have given the persistence exponent to the third decimal place. The nonlinear corrections are extremely weak for persistence and its behavior is dominated essentially by the persistence exponent.

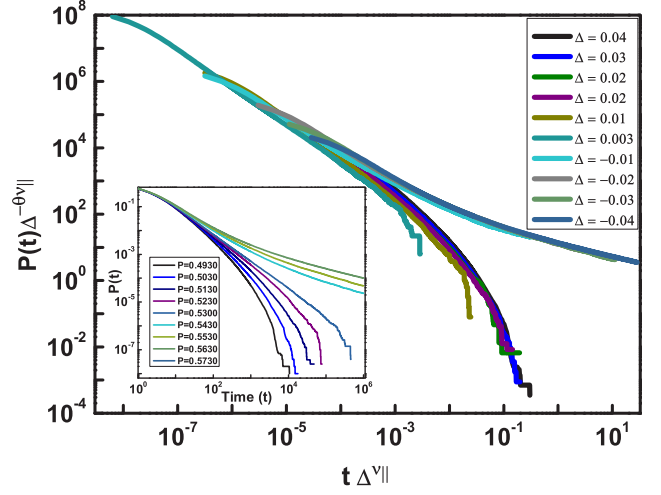


FIG. 15. Plot of $P(t)\Delta^{-\theta v_{||}}$ as a function of $t\Delta\theta_{||}^v$ for the IMD model at the critical point $p_c = 0.5330$ for various values of Δ .

Finally, we would like to comment on a delayed logistic map. Using a pseudospatiotemporal representation, phases and phase transitions can be defined in this model. It was conjectured by Lepri and later confirmed by Mahajan and Gade that this transition is indeed in the directed Ising class [27,53]. However, persistence (as defined above) does not act as a good order parameter for this system and there is no well-defined persistence exponent. The reason is simple. The system is updated in a sequential (typewriter) mode from left to right and has a one-sided coupling. Thus disturbances travel from left to right. Thus persistence goes to zero rapidly. However, for cases in which persistence acts as an alternative order parameter, the exponent is unity or very close to it.

V. CONCLUSION

We have demonstrated that for the directed Ising model in one dimension, the persistence exponent is universal and close

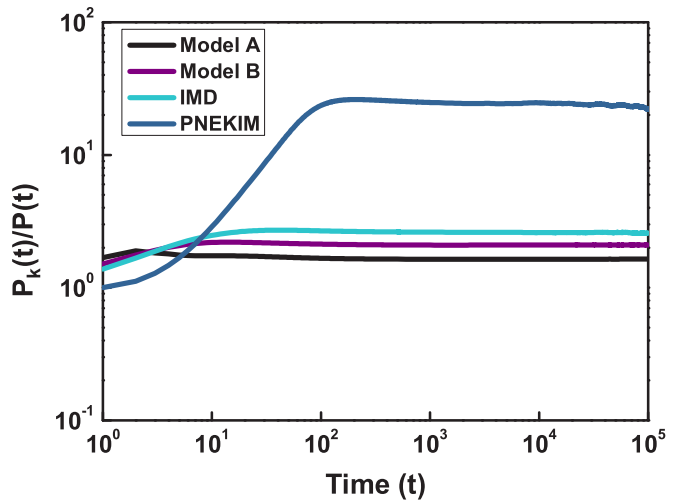


FIG. 16. Plot of $P_k(t)/P(t)$ as a function of t for Grassberger's models and the IMD model. For Grassberger's models, NEKIM with parallel update and the IMD model $k = 2$ and for the PNEKIM $k = 20$.

to unity. We have studied five different models in this context. We have also studied a generalization of persistence known as graded persistence, which has the same persistence exponent. We have also studied finite-size scaling in all models. We also studied off-critical scaling for persistence in some cases. It has been observed that excellent scaling collapse can be obtained using standard values for the directed Ising universality class. Thus further numerical evidence has been provided for the conjecture that persistence can be used as an alternate order parameter for the partially or completely frozen case. Given the nonuniversality of the persistence exponent in general, it

is interesting that a range of models has the same persistence exponent. These studies may shed more light on the dynamic process of the DI class.

ACKNOWLEDGMENTS

P.M.G. acknowledges the DST-SERB (Department of Science and Technology, India) Grant No. EMR/2016/006685 research scheme for financial assistance and the referees for useful suggestions.

-
- [1] D. Zhong and D. ben-Avraham, *Phys. Lett. A* **209**, 333 (1995).
 - [2] J. L. Cardy and U. C. Täuber, *J. Stat. Phys.* **90**, 1 (1998).
 - [3] J. Cardy and U. C. Täuber, *Phys. Rev. Lett.* **77**, 4780 (1996).
 - [4] T. M. Liggett, *Interacting Particle Systems*, Classics in Mathematics, Vol. 276 (Springer Science + Business Media, Berlin, 2012).
 - [5] I. Dornic, H. Chaté, J. Chave, and H. Hinrichsen, *Phys. Rev. Lett.* **87**, 045701 (2001).
 - [6] J. L. Cardy, *J. Phys. A: Math. Gen.* **16**, L709 (1983).
 - [7] J. L. Cardy and P. Grassberger, *J. Phys. A: Math. Gen.* **18**, L267 (1985).
 - [8] H. K. Janssen, *Z. Phys. B* **58**, 311 (1985).
 - [9] E. Domany and W. Kinzel, *Phys. Rev. Lett.* **53**, 311 (1984).
 - [10] J. Essam, *J. Phys. A: Math. Gen.* **22**, 4927 (1989).
 - [11] S. Manna, *J. Phys. A: Math. Gen.* **24**, L363 (1991).
 - [12] M. Henkel, H. Hinrichsen, and S. Lübeck, *Non-Equilibrium Phase Transitions* (Springer, Berlin, 2008), Vol. 1.
 - [13] G. Ódor, *Rev. Mod. Phys.* **76**, 663 (2004).
 - [14] P. Grassberger, H. Chaté, and G. Rousseau, *Phys. Rev. E* **55**, 2488 (1997).
 - [15] M. Muñoz, G. Grinstein, and R. Dickman, *J. Stat. Phys.* **91**, 541 (1998).
 - [16] A. Jiménez-Dalmaroni and H. Hinrichsen, *Phys. Rev. E* **68**, 036103 (2003).
 - [17] S. Lübeck and P. C. Heger, *Phys. Rev. E* **68**, 056102 (2003).
 - [18] I. Jensen, *Phys. Rev. Lett.* **70**, 1465 (1993).
 - [19] M. B. Matte and P. M. Gade, *J. Stat. Mech.* (2016) 113203.
 - [20] M. J. Howard and U. C. Täuber, *J. Phys. A: Math. Gen.* **30**, 7721 (1997).
 - [21] M. Henkel and H. Hinrichsen, *J. Phys. A: Math. Gen.* **37**, R117 (2004).
 - [22] F. Smallenburg and G. T. Barkema, *Phys. Rev. E* **78**, 031129 (2008).
 - [23] P. Grassberger, *J. Stat. Mech.* (2006) P01004.
 - [24] P. Grassberger, *Z. Phys. B* **47**, 365 (1982).
 - [25] N. Menyhárd and G. Ódor, *J. Phys. A: Math. Gen.* **30**, 8515 (1997).
 - [26] S. N. Majumdar, A. J. Bray, S. J. Cornell, and C. Sire, *Phys. Rev. Lett.* **77**, 3704 (1996).
 - [27] A. V. Mahajan and P. M. Gade, *Int. J. Bifurcat. Chaos* **29**, 1950066 (2019).
 - [28] P. Grassberger, F. Krause, and T. von der Twer, *J. Phys. A: Math. Gen.* **17**, L105 (1984).
 - [29] P. Grassberger, *J. Phys. A: Math. Gen.* **22**, L1103 (1989).
 - [30] S. Wolfram, *Cellular Automata and Complexity: Collected Papers* (CRC, Boca Raton, 2018).
 - [31] M. Bramson and L. Gray, *Z. Wahrscheinlichkeit.* **68**, 447 (1985).
 - [32] H. Park, M. H. Kim, and H. Park, *Phys. Rev. E* **52**, 5664 (1995).
 - [33] H. Park and H. Park, *Physica A* **221**, 97 (1995).
 - [34] W. M. Hwang and H. Park, *Phys. Rev. E* **59**, 4683 (1999).
 - [35] N. Menyhard, *J. Phys. A: Math. Gen.* **27**, 6139 (1994).
 - [36] B. Derrida, V. Hakim, and V. Pasquier, *J. Stat. Phys.* **85**, 763 (1996).
 - [37] G. I. Menon and P. Ray, *J. Phys. A: Math. Gen.* **34**, L735 (2001).
 - [38] P. M. Gade and G. G. Sahasrabudhe, *Phys. Rev. E* **87**, 052905 (2013).
 - [39] G. Y. Vichniac, *Physica D* **10**, 96 (1984).
 - [40] S. N. Majumdar, *Curr. Sci.* **77**, 370 (1999).
 - [41] D. Stauffer, *Eur. Phys. J. B* **30**, 587 (2002).
 - [42] H. Hinrichsen and H. M. Koduvely, *Eur. Phys. J. B* **5**, 257 (1998).
 - [43] E. V. Albano and M. A. Muñoz, *Phys. Rev. E* **63**, 031104 (2001).
 - [44] J. Fuchs, J. Schelter, F. Ginelli, and H. Hinrichsen, *J. Stat. Mech.* (2008) P04015.
 - [45] G. I. Menon, S. Sinha, and P. Ray, *Europhys. Lett.* **61**, 27 (2003).
 - [46] N. Menyhárd and G. Odor, *J. Phys. A: Math. Gen.* **29**, 7739 (1996).
 - [47] M. A. Saif and P. M. Gade, *J. Stat. Mech.* (2010) P03016.
 - [48] G. Manoj and P. Ray, *Phys. Rev. E* **62**, 7755 (2000).
 - [49] J. D. Noh and H. Park, *Phys. Rev. E* **69**, 016122 (2004).
 - [50] I. Jensen, *Phys. Rev. E* **50**, 3623 (1994).
 - [51] S.-C. Park, *J. Korean Phys. Soc.* **62**, 469 (2013).
 - [52] G. Ódor and N. Menyhárd, *Phys. Rev. E* **57**, 5168 (1998).
 - [53] S. Lepri, *Phys. Lett. A* **191**, 291 (1994).